JOURNAL OF GUIDANCE, CONTROL, AND DYNAMICS
Vol. 15, No. 2, March-April 1992

Performance Improvement of a Dynamically Tuned Gyroscope Using an Input Compensator

Taesam Kang, Jang Gyu Lee, and Chan Gook Park
Seoul National University, Seoul, Korea

An improved rebalance loop of a dynamically tuned gyroscope that has annexed an input compensator to the conventional rebalance loop is proposed in this paper. The input compensator is a simple estimator of input rates to the gyro, which is to be subtracted from torquing command. The improved rebalance loop significantly reduces transient torquing error, which allows higher gain and wider bandwidth loop as well as smaller tilt angle over transient state. Thus, it contributes to the accuracy improvement and widening dynamic range of the gyroscope. It is also shown that the stability robustness of the rebalance loop combined with the input compensator can be recovered by adjusting the bandwidth of the input compensator. Closed-loop frequency response analysis shows an improvement of the rebalance loop with the use of the input compensator, compared with a conventional one, in that the ratio between input and output torque has unity magnitude as well as low phase shift in wider range. The improved rebalance loop has been fabricated with analog devices and connected to a real gyroscope. The experiment result is compared with that of simulation. Both of them have demonstrated that the responses of output torque and rotor's tilt angle are considerably improved.

Nomenclature

A	= inertial moment of the rotor (including gimbal) along X_r and Y_r axes
B^H	= complex conjugate transpose of B
B^T	= transpose of B
B^{-1}	= inverse of B
$\det(B)$	= determinant of B
H	= angular momentum of rotor along the Z_r axis, $A \times \omega_{nu}$
I	= 2×2 identity matrix
$\underline{M}$	= $[M_x, M_y]^T$
$\underline{M}_i$	= $[M_{ix}, M_{iy}]^T$
M_{ix}, M_{iy}	= (negative) torque effects of the input rates along X_c and Y_c axes, respectively
M_x, M_y	= rebalance torques applied along X_c and Y_c axes, respectively
X_c, Y_c, Z_c	= case frame
X_r, Y_r, Z_r	= rotor-referenced frame
ζ	= damping coefficient of a dynamically tuned gyroscope
$\underline{\Theta}(s)$	= Laplace transform of $\underline{\theta}$
$\underline{\theta}$	= $[\theta_x, \theta_y]^T$
θ_x, θ_y	= tilt (or pickoff) angles between the rotor and the case of a dynamically tuned gyroscope
$\lambda(B)$	= eigenvalues of B
$\bar{\sigma}(B)$	= maximum singular value of $B \equiv \lambda_{max}^{1/2}(B^H B)$
$\underline{\sigma}(B)$	= minimum singular value of $B \equiv \lambda_{min}^{1/2}(B^H B)$
$\underline{\Phi}(s)$	= Laplace transform of $\underline{\phi}$
$\underline{\phi}$	= $[\phi_x, \phi_y]^T$
ϕ_x, ϕ_y	= input angles along X_c and Y_c axes, respectively

Taesam Kang was born on April 6, 1963, in Cheju Do, Korea. He received the B.S. and M.S. degrees in control and instrumentation engineering from Seoul National University, Seoul, Korea, in 1986 and 1988, respectively. He is presently a doctoral student in the Department of Control and Instrumentation Engineering of the Seoul National University. He is a research assistant at the Automation and Systems Research Institute, Seoul National University. His current research interests include the inertial navigation system and disturbance localization theory.

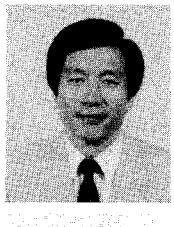

Jang Gyu Lee is the Associate Professor of the Department of Control and Instrumentation Engineering of Seoul National University. He received his B.S. degree from the Seoul National University, and M.S. and Ph.D. degrees from the University of Pittsburgh in 1971, 1974, and 1977, respectively. He worked for the Analytical Sciences Corporation in Reading, Massachusetts, and the Charles Stark Draper Laboratory in Cambridge, Massachusetts, before he joined the faculty of the Seoul National University in 1982. His current research interests include the inertial navigation system, vehicle parameter identification, and automated guided vehicle.

Chan Gook Park was born in Seoul, Korea, on September 13, 1961. He received the B.S. and M.S. degrees in control and instrumentation engineering from Seoul National University, Seoul, Korea, in 1985 and 1987, respectively. He is presently working toward the Ph.D. degree in the Department of Control and Instrumentation Engineering, Seoul National University. He is a research assistant at the Automation and Systems Research Institute, Seoul National University. His current research interests include the inertial navigation systems, Kalman filtering, and large scale systems.

Presented as Paper 90-3418 at the AIAA Guidance, Navigation, and Control Conference, Portland, OR, Aug. 20-22, 1990; received Oct. 23, 1990; revision received May 22, 1991; accepted for publication May 23, 1991.

ω_{fi} = cutoff frequency of the input compensator
ω_{nu} = nutation frequency $\equiv H/A$
$\equiv$ = equal by definition

Introduction

A DYNAMICALLY tuned gyroscope (DTG) is a two-degree-of-freedom gyroscope that, in principle, is based on the negative spring effect of a rotating gimbal or gimbals.[1] This DTG, the concept of which was arranged in the 1960s, began to be developed in the 1970s, and was utilized regularly in the 1980s, is widely accepted as a sensor for strapdown systems.[2-5,12]

The DTG consists of two major subassemblies: the mechanical part and the electrical part. The mechanical part consists of a case, a rotor, and a suspension system. The electrical part consists of a driving motor and rebalance loop that is composed of pickoffs, demodulators, low pass filters, notch filters, torquers, and compensators.

The rebalance loop controls the rotor, which is a sensing element, so that the tilt angles are kept small and the DTG is always in operating range. The performance of the rebalance loop plays an important role in determining the accuracy and the operating range of a DTG.

In a strapdown system, the DTG is mechanized as a sensor by using a regulator (or rebalance) loop to apply torques to the gyro rotor so that the angle between the rotor spin axis and gyro case (tilt angle) is nulled. The torque required to maintain null is proportional to the inertial rate that is applied to the gyro case when it is assumed that the null condition is retained. The dynamic errors of a DTG are directly affected by the magnitude of the tilt angle over transient state.[8,9]

Therefore, the strapdown system requires a good rebalance loop design to reduce the transient dynamic errors and to obtain a wide operating range. For a good performance, it is desired to have a low noise, robustly stable, wide bandwidth loop with regard to output torque vs input torque with low phase shift as well as unity magnitude and small tilt angle over transient state to reduce the dynamic errors.

Briggs[7] suggested a simple rule to design a stable rebalance loop for a general two-degree-of-freedom gyroscope. Digital control of a DTG is suggested by Steel and Puri[14] and Coffman.[6] Recently, Constancis and Sorine[15] applied linear quadratic Gaussian (LQG) methodology to design a rebalance loop and showed by simulation and experiment that a wide bandwidth rebalance loop can be achieved.

Previous works[6,7,14] in designing a rebalance loop considered the input rates to the DTG as external disturbances that are to be compensated through feedback. LQG design is somewhat complex to be implemented in an analog system.

This paper proposes an input compensator to precompensate the disturbance effects of the input rates of the DTG by including it in the rebalance loop, extending the bandwidth of the rebalance loop wider than a simple proportional, integral, derivative (PID) controller can do while it retains the stability robustness of the loop. This design method is somewhat like LQG[15,16] or LQG/loop transfer recovery (LTR)[10] methodologies. But the structure of the proposed method is simpler than that of an LQG or LQG/LTR based rebalance loop, which enables simple analog implementation. The idea of adding an input compensator to the rebalance loop is primarily developed for DTG in this paper. However, the idea can be extended easily to any gyroscope including a single-degree-of-freedom (SDF) gyroscope.[13] The performance improvement of DTGs employing the input compensator is verified through frequency response analysis, simulation, and experiment with the Seoul National University (SNU)-DTG, which is designed and fabricated at Seoul National University.[5]

Dynamically Tuned Gyroscope Model

A schematic of the sensing part of the DTG and coordinate frames are shown in Fig. 1. The X_c Y_c Z_c set is the case frame that is fixed to the case of the DTG. The Z_c axis coincides with

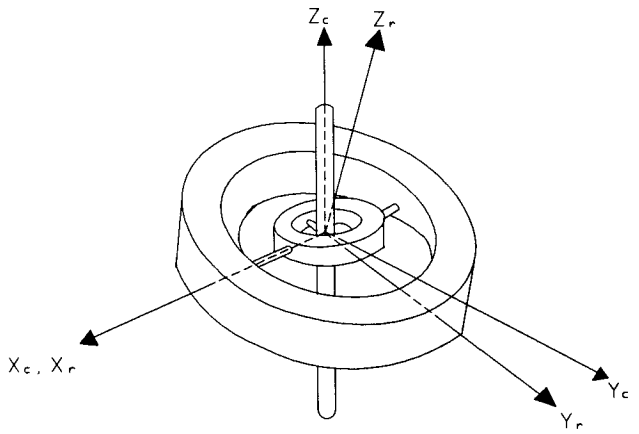

Fig. 1 Definition of the coordinate frames.

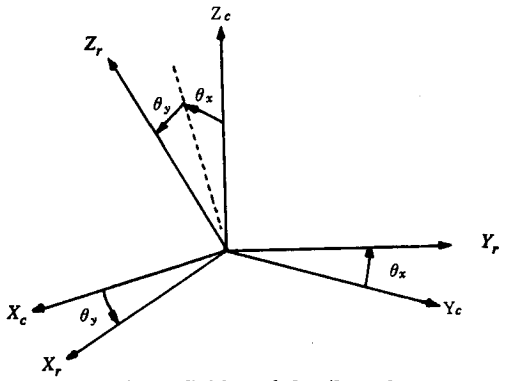

Fig. 2 Definition of the tilt angles.

the spin axis of the shaft, which is connected to the rotation axis of the driving motor. The coordinate set X_r Y_r Z_r is the rotor-referenced frame. Axes X_r and Y_r are on the plane of the rotor (not fixed to it) and the Z_c axis coincides with an instantaneous rotor spin axis. Note that the rotor-referenced frame does not spin with the rotor along the Z_r axis. The instantaneous attitude of the DTG's rotor with respect to the case frame is specified by the tilt angles θ_x, θ_y, as shown in Fig. 2.

When small tilt angles (less than 0.5 deg), symmetrical structure, tuned condition, and low damping are assumed and small error terms are ignored, the dynamic equation that describes a DTG input-output relationship in Laplace transform is given by the following equations[6-9]:

$$\underline{\Theta}(s) = \frac{1}{s} G_s(s)\underline{M}(s) - \underline{\Phi}(s) \tag{1}$$

where

$$G_s(s) \equiv \frac{1}{A(s^2 + 2\zeta\omega_{nu}s + \omega_{nu}^2)} \begin{bmatrix} s & -\omega_{nu} \\ \omega_{nu} & s \end{bmatrix} \tag{2}$$

Equations (1) and (2) are used as a DTG model to design a rebalance loop. In SNU-DTG, A, ω_{nu}, and ζ are 4.67305×10^{-5} kgm^2, 764.2009 rad/s, and 1.4×10^{-3}, respectively. The spin frequency is 418.9 rad/s.

Design of a Rebalance Loop Using an Input Compensator

General rebalance loop design methods can be found in other works.[5-7] In this section, the noninteractive-control-based rebalance loop design using the PID scheme will be briefly explained first, and then the improvement of the rebalance loop using an input compensator will be proposed, which is the main subject of this paper.

The noninteractive control uses the well-known principles of noninteraction,[6] in which the matrix of the open-loop transfer function is decoupled. In DTG rebalance loop design, this

principle can be applied simply by inserting the circuit given by Eq. (3) in the rebalance loop, which in fact acts as a nutation damping circuit:

$$N(s) = \begin{bmatrix} 1 & -\dfrac{s}{\omega_{nu}} \\ \dfrac{s}{\omega_{nu}} & 1 \end{bmatrix} \tag{3}$$

Now, the DTG system with decoupling circuit inserted can be assumed to be two independent single-input, single-output (SISO) systems and a standard SISO control scheme can be applied. But the complete decoupling is impossible; therefore, the final check for stability must be done with the undecoupled model.

In common DTG designs, the tilt angle signal is modulated on a carrier. The modulated signal must be demodulated and low pass filtered to retrieve the tilt angle and attenuate the carrier. To reduce gyro spin frequency noise, a notch filter is used or bandwidth is limited.

In SNU-DTG, the carrier signal is a 38.4-kHz sine wave and a low pass filter of bandwidth about 200 rad/s is used. The s term in the decoupling circuit is approximated by $d_n(s)$, which acts as a derivative operator in low-frequency range, which is the pass band of the DTG, and rejects high-frequency noises including the carrier signal:

$$d_n(s) = \frac{s}{[(s/3000) + 1][(s/4000) + 1]} \tag{4}$$

Figure 3 is a simple block diagram of the rebalance loop of the SNU-DTG. In the figure, the dotted part is the input compensator block, which will be explained later. At this point, we will start with the part of the PID scheme rebalance loop. The low-pass filter $G_f(s)$ and the PID compensator $G_c(s)$ used in the SNU-DTG rebalance loop are

$$G_f(s) = \frac{1}{(s^2/\omega_f^2) + 2(\zeta_f/\omega_f) + 1} I \tag{5}$$

$$G_c(s) = k\left(\frac{s\tau_1 + 1}{s(s\tau_2 + 1)} + k_d d(s)\right)\begin{pmatrix} 1 & \dfrac{-d_n(s)}{\omega_{nu}} \\ \dfrac{d_n(s)}{\omega_{nu}} & 1 \end{pmatrix} \tag{6}$$

where $k = 8$, $\omega_f = 200$ rad/s, $\zeta_f = 1.247$, $\tau_1 = 0.1$, $\tau_2 = 1.1805 \times 10^{-4}$, $k_d = 0.001$, and $d(s)$ is given in Eq. (7):

$$d(s) = \frac{1}{[(s/500) + 1][(s/6667) + 1]} \tag{7}$$

For open-loop frequency analysis, the path between θ_x and the compensator $G_c(s)$ is broken. Figure 4 is the open-loop bode plot. Figure 5 is the closed-loop frequency response between $\dot{\phi}_y$ and M_x. In both cases, the responses of the other axis are similar. In the figures, the straight lines represent PID scheme frequency responses and the dotted lines represent the improved frequency responses using input compensator whose descriptions follow. Figure 4 shows that the gain and phase margin of the PID-based rebalance loop is about 15 dB and 65 deg, respectively.

Now, we design an input compensator and attach it to the existing rebalance loop to improve its performance. The torques that are the outputs of rebalance loop and the input rates that are measured by a DTG are the main factors that dominate the motion of the DTG's rotor. The input rates act as disturbances to the rebalance loop. However, the disturbance effects of the input rates can be eliminated with the design of an input compensator, which is explained later. When the disturbance effects of the input rates are eliminated, the rotor acts as if there were no input rates, i.e., the rotor acts as if there were no disturbances and an ideal regulator or an ideal rebalance loop is realized.

In the first step, an "input observer," which is described in Eq. (8), is generated by simply reformulating Eq. (1):

$$\underline{\dot{\Phi}}(s) = G_s(s)\underline{M}(s) - \underline{\dot{\Theta}}(s) \tag{8}$$

Since $M(s)$ is the output of rebalance loop, and A , ζ, and ω_{nu} are the design parameters of the DTG rotor, Eq. (8) can be solved for $\underline{\dot{\Phi}}(s)$ by simply differentiating the tilt angle $\underline{\Theta}(s)$. The $\underline{\dot{\Phi}}(s)$ can be obtained using an optimal filter or the other observers, but the structures of them are somewhat complex to be implemented with analog devices.

Let $M_i(s)$ be the (negative) torquing effect of the input rate applied to DTG along the X_r and Y_r axes. To see the torquing effect from the DTG input, if we assume that $\underline{\dot{\Theta}}(s)$ is zero and ignore the rotor damping ζ in Eq. (8), $\underline{M}_i(s)$ can be obtained

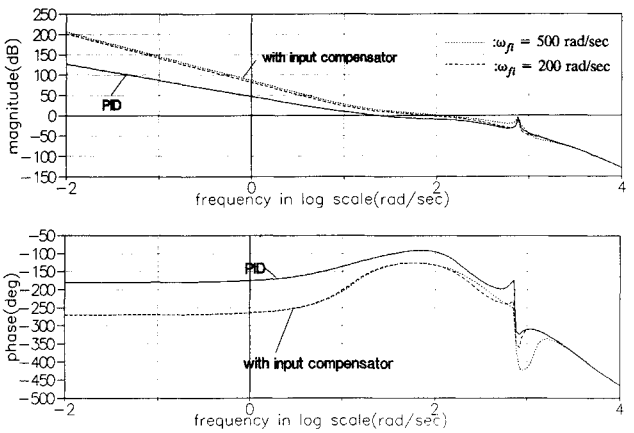

Fig. 4 Open-loop frequency responses.

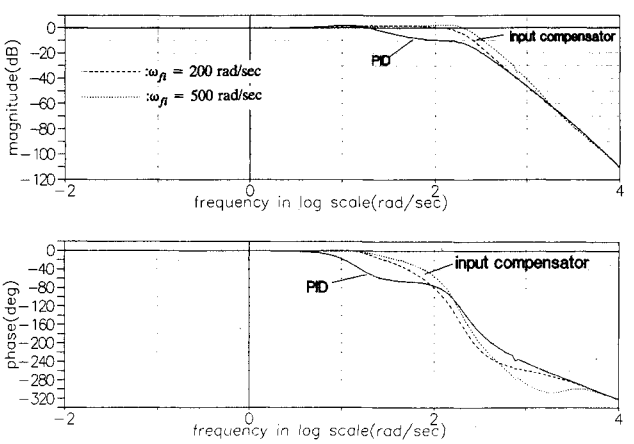

Fig. 5 Closed-loop frequency responses.

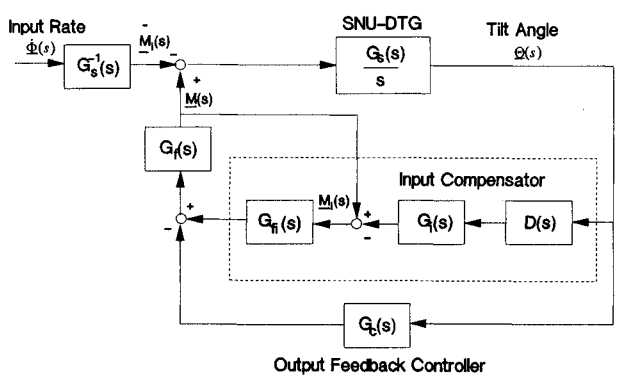

Fig. 3 Block diagram of the rebalance loop with the input compensator.

by solving for $\underline{M}(s)$. They are summarized in the following equation:

$$\underline{M}_i(s) = G_i(s)\dot{\underline{\Phi}}(s) \tag{9}$$

where

$$G_i(s) \equiv \begin{bmatrix} As & H \\ -H & As \end{bmatrix} \tag{10}$$

Equations (8–10) can be rewritten in a simple form:

$$\underline{M}_i(s) = \underline{M}(s) - G_i(s)\dot{\underline{\Theta}}(s) \tag{11}$$

Equation (11) provides the basis for designing the input compensator, and it is depicted in Fig. 3 in block diagram form. In the figure, $\underline{\tilde{M}}_i(s)$ is the true torque effect of input rate, whereas $\underline{M}_i(s)$ is an estimate of $\underline{\tilde{M}}_i(s)$ obtained from the input observer. To calculate $\dot{\underline{\Theta}}(s)$ from $\underline{\Theta}(s)$, a differentiator block $D(s) \equiv d(s)I$ is added. In other words, since the tilt angle $\underline{\theta}$ is measured and the derivative of it is not measured directly from SNU-DTG, $\dot{\underline{\Theta}}(s)$ is approximated by $D(s)\underline{\Theta}(s)$.

Without the input compensator, the transfer function $T(s)$ between $\dot{\underline{\Phi}}(s)$ and $\underline{\Theta}(s)$ is given by

$$T(s) = -\frac{1}{s}\left(I + \frac{G_s(s)}{s}G_f(s)G_c(s)\right)^{-1} \tag{12}$$

Noting the block symmetric property of the DTG system,[16] the closed-loop transfer function including the input compensator is given by Eq. (13):

$$T_c(s) = -\frac{1}{s}\left[I + \Xi(s) + \frac{G_s(s)}{s}G_f(s)G_c(s)\right]^{-1} \times [I - G_f(s)G_{fi}(s)] \tag{13}$$

where

$$\Xi(s) = G_f(s)G_{fi}(s)\left(G_s(s)G_i(s)\frac{D(s)}{s} - I\right) \tag{14}$$

In the equations for the input compensator, $G_{fi}(s)$ is a low pass filter inserted for noise reduction. It also contributes to the stability of the rebalance loop with input compensator, which will be explained later. The $G_{fi}(s)$ used in the SNU-DTG rebalance loop is

$$G_{fi}(s) = \frac{1}{(s^2/\omega_{fi}^2) + 2(\zeta_{fi}/\omega_{fi}) + 1}I \tag{15}$$

where $\zeta_{fi} = 1.2$ and $\omega_{fi} = 200$ rad/s. The damping coefficient ζ_{fi} can be used to shape the response of the input compensator. In realizing $G_i(s)$, the term As is also approximated by $Ad(s)$. In fact, the magnitude of the term As is very small compared with that of the term H in low-frequency range, and therefore, the term As can be ignored from $G_i(s)$.

In the low-frequency range, $G_f(s)$ and $G_{fi}(s)$ are approximately equal to I and $G_i(s)G_s(s)$ is also approximately I, which implies that the ratio between $T_c(s)$ and $T(s)$ is approximately zero in the normal operating range of a DTG, which says that the input compensator eliminates disturbance effects of input rates more effectively compared with the conventional PID loop. For stability, $G_{fi}(s)$ should be designed that the magnitude of $\Xi(s)$ be small compared with that of $[G_s(s)/s]G_f(s)G_c(s)$ in the high-frequency range where the approximations employed in designing the input compensator do not hold, which makes the total loop satisfy stability conditions. For this reason, the pass band of $G_{fi}(s)$ should be less than that of $D(s)$. In the meantime, the other controller (PID controller) maintains stability, i.e., it extenuates remaining disturbances which have not been eliminated by the input compensator due to parameter errors and the other noise. Again, Figs. 4 and 5 show the open-loop and closed-loop frequency responses, respectively. Figure 4 shows that the proposed loop has higher gain in the performance region of the DTG and approximately the same in the high frequency region with little stability degradation, which enables higher gain, wider bandwidth loop, as well as smaller tilt angle over the transient state to be achieved beyond those that are possible with a simple PID controller, improving the performance of a DTG. Figure 5 also shows the performance improvement of the loop with the input compensator, compared with the PID based one, in that the ratio between input and output torque has unity magnitude and low phase shift in a wider region.

Effect of the Input Compensator on Stability

After an input compensator is employed in the rebalance loop, stability robustness of the rebalance loop should not be damaged because of the input compensator. In this section, the effect of the input compensator on stability robustness of the rebalance loop and the conditions that the stability be retained are presented.

Consider a perturbed system $G_p(s)$ as follows:

$$G_p(s) \equiv E(s) + G(s) \tag{16}$$

where $E(s)$ is a perturbation term, which is restricted as

$$\bar{\sigma}[E(j\omega)] \le M(\omega), \qquad 0 \le \omega \le \infty \tag{17}$$

Assume that 1) $G(s)[I + G(s)]^{-1}$ is stable; 2) $G_p(s)$ in Eq. (16) remains to be a strictly proper finite-dimensional linear time-invariant system and $G_p(s)$ has the same number of unstable modes as $G(s)$; 3) $G(s)$ has no pole on the imaginary axis, except the zero point, of the complex plane; and 4) $E(s)$ is continuous.

Let's first find the condition that the stability of the perturbed system be retained. Under these conditions, the following lemma holds.[10]

Lemma 1: The closed system $G_p(s)[I + G_p(s)]^{-1}$ is stable if

$$\text{i) } \underline{\sigma}[I + G(j\omega)] > M(\omega), \qquad \text{for all } \omega \ne 0 \tag{18}$$

$$\text{ii) } \lim_{r\to 0} \underline{\sigma}[I + G(re^{j\theta})] > \lim_{\omega\to 0} M(\omega), \quad (-90 \text{ deg} \le \theta \le 90 \text{ deg}) \tag{19}$$

Proof: According to the multivariable Nyquist criteria,[10,11] the condition for the stability of the system $G(s)[I + G(s)]^{-1}$ is that the encirclement count of the map $\det[I + G(s)]$, evaluated on the standard Nyquist D contour, be equal to the (negative) number of unstable open-loop modes of $G(s)$.

Similarly, for the system $G_p(s)[I + G_p(s)]^{-1}$ to be stable, the number of encirclements of the map $\det[I + G_p(s)]$ must equal the (negative) number of unstable modes of $G_p(s)$, however, this number is the same as that of encirclements of $\det[I + G(s)]$. Hence, the stability condition of $G_p(s)[I + G_p(s)]^{-1}$ is satisfied if and only if the number of encirclements of $\det[I + G_p(s)]^{-1}$ remains unchanged for all $G_p(s)$ allowed by Eqs. (16) and (17). This is assured if and only if $\det[I + G_p(s)]$ remains nonzero as $G(s)$ is warped continuously toward $G_p(s)$, i.e.,

$$\det[I + \epsilon E(\bar{s}) + G(\bar{s})] \ne 0 \tag{20}$$

for all $0 \le \epsilon \le 1$, all $\bar{s}$ on the D contour, and all $E(s)$ satisfying Eq. (17). Since $G_p(s)$ vanishes on an infinite radius segment of D contour, Eq. (20) is equivalent to Eq. (21):

$$\det[I + \epsilon E(j\omega) + G(j\omega)] \ne 0$$

$$\lim_{r\to 0} \det[I + \epsilon E(re^{j\theta}) + G(re^{j\theta})] \ne 0 \tag{21}$$

for all $0 \le \epsilon \le 1$, all $\omega \ne 0$, all $E(s)$ satisfying Eq. (17), and all -90 deg $\le \theta \le 90$ deg. This is satisfied if

$$\underline{\sigma}[I + G(j\omega)] > M(\omega)$$

$$\lim_{r\to 0} \underline{\sigma}[I + G(re^{j\theta})] > \lim_{r\to 0} \bar{\sigma}[E(re^{j\theta})] \tag{22}$$

for all $\omega \ne 0$, all $E(s)$ satisfying Eq. (17), and all -90 deg $\le \theta \le 90$ deg. Equations (17) and (22) prove the lemma.

Now, the stability of the rebalance loop with the input compensator can be proved. Assume that the rebalance loop without the input compensator is stable. The following theorem proves the stability.

Theorem 1: The stability of the rebalance loop with the input compensator given by Eqs. (13) and (14) is kept if

$$\text{i) } \underline{\sigma}\left(I + \frac{G_s(j\omega)}{j\omega} G_f(j\omega)G_c(j\omega)\right) > \bar{\sigma}[\Xi(j\omega)] \tag{23}$$

$$\text{ii) } \lim_{r\to 0} \underline{\sigma}\left[I + \frac{G_s(re^{j\theta})}{re^{j\theta}} G_f(re^{j\theta})G_c(re^{j\theta})\right] > \lim_{\omega\to 0} \bar{\sigma}[\Xi(j\omega)] \tag{24}$$

for all $\omega \ne 0$ and all -90 deg $\le \theta \le 90$ deg.

Proof: Let $G(s) = [G_s(s)/s]G_f(s)G_c(s)$, $E(s) = \Xi(s)$, and $M(\omega) = \bar{\sigma}[\Xi(j\omega)]$. Then, lemma 1 proves the theorem.

For practical purposes, it is the stability robustness rather than stability itself that is important. Now it will be shown that the stability robustness of the loop with the input compensator can be retained or recovered by adjusting the bandwidth of the low pass filter $G_{fi}(s)$. In Eqs. (12) and (13), the terms

$$\left(I + \frac{G_s(s)}{s} G_f(s)G_c(s)\right)^{-1}$$

and

$$\left[I + \Xi(s) + \frac{G_s(s)}{s} G_f(s)G_c(s)\right]^{-1}$$

determine the stability robustnesses of the PID controller loop and that of the proposed loop, respectively. But these terms can be made approximately equal by limiting the bandwidth of the $G_{fi}(s)$ less than that of $D(s)$ as explained before. This is somewhat like loop transfer recovery in LQG/LTR methodology as far as stability robustness is concerned. Figure 4 shows that the stability robustness is recovered as the bandwidth of the $G_{fi}(s)$ is limited. In the figure, the gain of the loop with the input compensator is greater than that of the PID loop in the low-frequency range, which is the performance region of the DTG. But they are approximately equal in the high-frequency region where stability of the loop is determined. Therefore, the performance of the loop is improved with little stability robustness degradation.

Experiment and Simulation Results

The performance improvement of the proposed loop is affirmed through simulation and experiment with analog circuits using the SNU-DTG.

An experimental input compensator is designed and included in the analog rebalance loop of the SNU-DTG in order to affirm the improvement of the rebalance loop. The step input rate of -2.5 deg/s applied along the X_c axis is used as a test input. Figure 6 compares the tilt angle response of PID loop and that of the proposed loop. In the SNU-DTG, the tilt angle is modulated on a carrier of a 38.4-kHz sine wave, as explained before. Therefore, a demodulator and a low pass filter are used to retrieve the signal of the tilt angle. The figure shows that the proposed loop cancels out the disturbance effect of the input rate; consequently, the tilt angle is kept very small compared with that of the conventional PID loop. This affirms the performance improvement of a DTG by reducing dynamic errors in a real environment. A little remnant shown

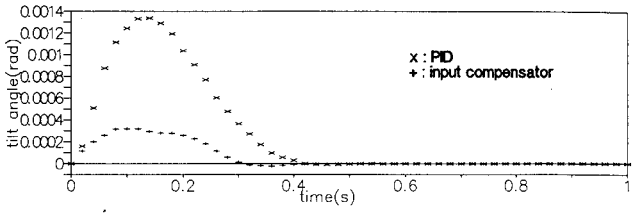

Fig. 6 Step responses (experiment).

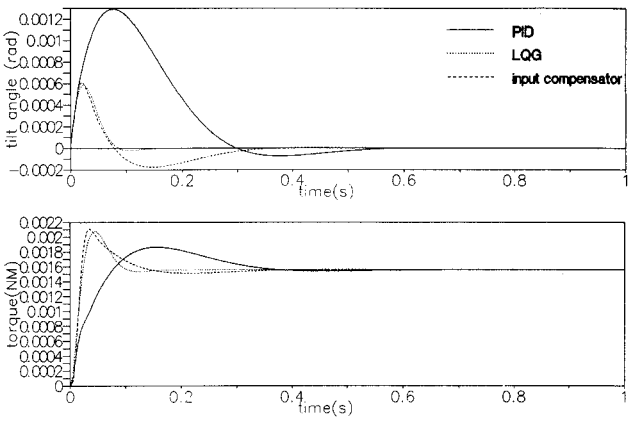

Fig. 7 Step responses (simulation).

in the figure is due to the low pass filters inserted for noise reduction and approximations of $\dot{\Theta}(s)$ and $G_i(s)$ in the loop. The oscillations, which could be occurring in the proposed loop response, can be reduced by adjusting the damping coefficient of the low pass filter $G_{fi}(s)$. The oscillation becomes smaller as the damping coefficient becomes larger.

Simulation tests are also included in the paper in order to compare the proposed scheme with the LQG scheme. The same test input used in the experiment is applied. Figure 7 shows the tilt angle and output torque responses of the PID, the PID with the input compensator, and LQG rebalance loops. The bandwidth of the LQG rebalance loop is adjusted to be the same as that of the proposed loop. The simulation result also shows that the tilt angle of the proposed loop is much smaller than that of the PID loop, as expected. The slight difference between experiment and simulation is mainly due to the low pass filter, which is used to retrieve the tilt angle signal. The figure also shows that the output torque of the proposed loop reaches the input rate much faster than the PID loop. This demonstrates the performance improvement of the proposed loop. In the figure, the LQG rebalance loop also works well, but the LQG loop is somewhat complex to be implemented in an analog system. On the other hand, the performance of the PID rebalance loop with the input compensator is approximately equal to that of the LQG loop, and the structure of the former is simpler than that of the latter. Therefore, it can be concluded that the rebalance loop of the PID with the input compensator is the best to implement an analog rebalance loop of a DTG.

Conclusions

An input compensator improving the performance of the rebalance loop of dynamically tuned gyroscopes has been devised, and it is illustrated that the compensator can improve the transient response of the rebalance loop. The main idea is that, in the conventional rebalance loop using a PID controller, the input to a gyroscope is treated as external disturbance; however, the input can be estimated and compensated, thus removing its effect in the rebalance loop. That is what the input compensator does, which allows a higher gain and a wider bandwidth loop as well as a smaller tilt angle over the transient state beyond those that are possible with a simple

PID controller. The open-loop frequency response showed that the loop with the input compensator has large gain in the performance region, improving performance of it while it has a small one (approximately equal to that of PID alone), keeping the stability robustness of the complete loop. The closed-loop frequency response showed that the proposed loop has better (torque) input/output response in that it has unity magnitude as well as low phase shift in a wider region compared with the conventional PID loop. Next, the condition that the annexed input compensator does not break the stability of the complete loop is proved and it is also shown that the stability robustness of the loop with the input compensator can be retained or recovered by adjusting the bandwidth of the input compensator, solving the stability robustness problem when it is to be used in a real environment. The input compensator can be applied also to a single-degree-of-freedom gyroscope to improve its performance. The experiment result of the proposed rebalance loop applied to a real gyroscope has demonstrated its performance improvement because the input compensator effectively eliminates disturbance effect of input rate. In simulation, the step responses of the rebalance loops of PID, PID with input compensator, and LQG are compared. The simulation result has also demonstrated the performance improvement of the proposed loop. The LQG loop is complex, whereas its performance is similar to the much simpler proposed rebalance loop. In conclusion, a rebalance loop combining PID and the input compensator is the most recommendable for a dynamically tuned gyroscope.

Acknowledgment

This work was supported by the Ministry of Science and Technology of Korea under the Special Project Program.

References

[1]Howe, E. W., and Savet, P. H., "The Dynamically Tuned Free Rotor Gyro," *Control Engineering,* Vol. 11, No. 6, 1964, pp. 67–72.

[2]Garg, S. C., Morrow, L. D., and Mamen, R., "Strapdown Navigation Technology: A Literature Survey," *Journal of Guidance and Control,* Vol. 1, No. 3, 1978, pp. 161–172.

[3]Carroll, R., "Inertial Technology for the Future," *IEEE Transactions on Aerospace and Electronic Systems,* Vol. AES-20, No. 4, 1984, pp. 425,426.

[4]Craig, R. J. G., "Theory of Operation of an Elastically Supported, Tuned Gyroscope," *IEEE Transactions on Aerospace and Electronic Systems,* Vol. AES-8, No. 3, 1972, pp. 280–288.

[5]Lee, J. G., "Development of Analytic Tools for Fabricating High Precision Instrument—Based on Building a Strapdown Inertial Navigation System," Seoul National University, Seoul, Korea, Aug. 1989.

[6]Coffman, D. E., "Feasibility Study of a Digital Rebalance Loop for a Dry Tuned TDF Gyro," NASA-CR-144089, May 1974, pp. 1–74.

[7]Briggs, R. W., "Stability of a Two-Degree-of-Freedom Gyro with External Feedback," *IEEE Transactions on Automatic Control,* Vol. AC-10, No. 3, 1965, pp. 244–249.

[8]Craig, R. J. G., "Dynamically Tuned Gyros in Strapdown Systems," NATO AGARD Paper 116, *Conference Proceedings on Inertial Navigation Components and Systems,* Florence, Italy, Oct. 1972.

[9]Bortz, J. E., "Dynamic Errors in a Tuned Flexure-Mounted Strapdown Gyro," Analytic Sciences Corporation, TR-147-5, Reading, MA, Sept. 1972.

[10]Doyle, J. C., and Stein, G., "Multivariable Feedback Design: Concepts for a Classical/Modern Synthesis," *IEEE Transactions on Automatic Control,* Vol. AC-26, No. 1, 1981, pp. 4–16.

[11]Rosenbrock, H. H., "The Stability of Multivariable Systems," *IEEE Transactions on Automatic Control,* Vol. AC-17, No. 1, 1972, pp. 105–107.

[12]Nurse, R. J., Prohaska, J. T., and Riegsecker, D. G., "A New Baseline for the Inertial Navigation Strapdown Simulator Program," Charles Stark Draper Lab., R-1136, Cambridge, MA, July 1978.

[13]Kang, T., and Lee, J. G., "Performance Improvement of a Single-Degree-of-Freedom Gyroscope Using an Input Compensator," *Journal of the Korean Society for Aeronautical and Space Sciences,* Vol. 18, No. 4, 1990, pp. 87–93.

[14]Steel, G. K., and Puri, S. N., "Direct Digital Control of Dry-Tuned Rotor Gyros," *Automatic Control in Space,* Vol. 2, edited by C. W. Munday, Pergamon, Oxford, England, UK, 1979, pp. 79–85.

[15]Constancis, P., and Sorine, M., "Wideband Linear Quadratic Gaussian Control of Strapdown Dry Tuned Gyro/Accelerometers," AIAA Paper 89-3441, *Proceedings of the AIAA Guidance, Navigation, and Control Conference,* AIAA, Washington, DC, 1989, pp. 141–145.

[16]Johnson, B. G., "Active Control of a Flexible, Two-Mass Rotor: The Use of Complex Notation," Ph.D. Dissertation, Massachusetts Inst. of Technology, Cambridge, MA, Sept. 1986.